Beltrán, Juan Carlos et al.

Article

Comparative analysis of deterministic and probabilistic methods for the integration of distributed generation in power systems

Energy Reports

Provided in Cooperation with:
Elsevier

Suggested Citation: Beltrán, Juan Carlos et al. (2020) : Comparative analysis of deterministic and probabilistic methods for the integration of distributed generation in power systems, Energy Reports, ISSN 2352-4847, Elsevier, Amsterdam, Vol. 6, Iss. 3, pp. 88-104, https://doi.org/10.1016/j.egyr.2019.10.025

This Version is available at:
https://hdl.handle.net/10419/243983

Available online at www.sciencedirect.com
ScienceDirect
Energy Reports 6 (2020) 88–104
www.elsevier.com/locate/egyr

Tmrees, EURACA, 04 to 06 September 2019, Athens, Greece

Comparative analysis of deterministic and probabilistic methods for the integration of distributed generation in power systems

Juan Carlos Beltrán[a], Andrés Julián Aristizábal[a,*], Alejandra López[b], Mónica Castaneda[a], Sebastián Zapata[a], Yulia Ivanova[c]

[a] *Engineering Department, Universidad de Bogotá Jorge Tadeo Lozano, Cr. 4 #22-61, Bogotá 110311, Colombia*
[b] *Environmental Science, Utah Valley University, 800W University Pkwy, Orem, UT 84057, United States of America*
[c] *Faculty of Engineering, Universidad Militar Nueva Granada, Cr. 11 #101-80, Bogotá 110311, Colombia*

Received 19 September 2019; accepted 25 October 2019
Available online 4 November 2019

Abstract

In this article, a comparative analysis is made between three statistical methods (Taguchi's Orthogonal Array Testing method, Monte Carlo and Two-Point method) by integrating the uncertainty of primary sources of renewable generation in systems of electric power. The modeling of the Institute of Electrical and Electronics Engineers test system of 13 nodes is made by integrating the distributed generation with two different sources: wind and photovoltaic. For the simulation of wind power generation, the wind speed data is from El Cabo de la Vela in the Guajira department in Colombia and for the simulation of solar power generation, the solar radiation data is from Bogota city in Colombia. Once the system of 13 nodes is modeled and incorporated to the variability of primary resource and the load in each case; the load flow can be made by using the Matpower tool in Matlab for each one of the statistical methods proposed. The voltage, power generated, and power demanded data is recovered for each method to create comparison charts, establish the advantages, and disadvantages of each one in the analysis of the distribution of power systems with distributed generation. The main results are: the Taguchi's Orthogonal Array Testing method improves its behavior if the number of levels is increased for each variable; more iterations in the Montecarlo method produce a greater precision of the probabilities; and the two-point method is a combination between the benefits of the deterministic and the probabilistic.

Peer-review under responsibility of the scientific committee of the Tmrees, EURACA, 2019.

Keywords: Distributed generation; Solar power; Wind power; Deterministic methods; Probabilistic methods

1. Introduction

Competitive electricity power system is based on a deregulated market structure consisting of electricity supplier and consumer transactions, coordination and rules that serve to guarantee competition and non-discriminatory open access [1].

* Corresponding author.
E-mail address: andresj.aristizabalc@utadeo.edu.co (A.J. Aristizábal).

https://doi.org/10.1016/j.egyr.2019.10.025

Peer-review under responsibility of the scientific committee of the Tmrees, EURACA, 2019.

Nomenclature

IEEE	Institute of electrical and electronics engineers
DG	Distributed generation
TOAT	Taguchi's orthogonal array testing method
PV	Photovoltaic
RES	Renewable energy sources
WTs	Wind turbines
PVs	Photovoltaic systems
PDF	Probability distribution function
OM	Orthogonal matrix
k	Shape parameter
c	Scale parameter
p.u.	Per unit

Photovoltaic (PV) power generation has rapidly developed as one of the world's most promising sources of energy [2]. A key aspect for high PV system penetration is financial viability, the assessment of which is dependent on a reliable prediction of the lifetime energy output of the system [3]. The solar PV power output depends on the ambient weather conditions such as incident solar radiation, temperature, humidity etc. As the weather parameters are themselves quite uncertain, the solar PV power also becomes uncertain in nature [4].

Increasing penetration of wind power raises concerns about un-certainties of the wind power generation. The uncertainties are related to the value and reliability of wind power generation as well as the variations of generation patterns [5]. The power generated by wind turbines is characterized by its power curve which shows the relationship between wind speed and its power output [6].

Distributed systems mean distributed processing in a shared environment to minimize computing time and to increase the overall performance [7]. In literature it has been proven that distributed energy systems offer multiple benefits and can become the norm of future energy systems, providing energy with low total annual cost and lower carbon emissions compared to conventional energy systems [8]. Modern power systems with increased integration of Renewable Energy Sources (RES), such as Wind Turbines (WTs) and Photovoltaic Systems (PVs) [9] introduce additional uncertainties in the power injections into the system due to their volatile primary sources throughout the year [10].

The loads on the distribution system vary instantaneously owing to the uncertainty of the power demand at the user end thus loads are assumed as random variables and are modeled using probability distribution functions [11]. Probabilistic power flow technique is a desirable method for evaluating the operating state of the electricity network under the uncertain environment [12]. Uncertain demands can be predicted by assigning proper probability distribution functions, which describe the uncertainties, to certain demands [13].

In the literature there are different studies to optimize energy systems using the Taguchi Method (TOAT) [14–16], for photovoltaic energy, thermal solar energy and wind energy. In this study we use the Montecarlo Method and the Two-Point Method in addition to the TOAT Method, to evaluate the impact of distributed generation on power systems.

2. Probabilistic and deterministic methods

2.1. Montecarlo simulation method

The Montecarlo simulation method is the one in which the properties of the distributions if the random variables are investigated by the simulation of aleatory numbers. This method is like the usual statistical methods if we leave aside the origin of the data, is in which aleatory samples are used to make inferences about the origin population. Generally, in its statistical application, a model is used to simulate a phenomenon that contains an aleatory component. In the Montecarlo method, on the other hand, the object of the investigation is a model based on itself and it used aleatory or pseudo-aleatory events are used to study.

Therefore, to be able to reach values of the reliability coefficients of the system, it is necessary to perform a simulation during determined time intervals. There are two types of techniques for simulation, deterministic and non-deterministic. The Montecarlo method is a numerical technique to calculate probabilities and other related amounts, using sequences of aleatory numbers.

For cases with a single variable the procedure is the following:

- Generate a series of aleatory numbers r1, r2, . . . , rm, evenly distributed in the range [0,1].
- Use this sequence to generate other sequence, x1, x2, . . . , xm, distributed according to the probability distribution function (PDF) to describe the aleatory variable.
- Use the sequence of x values to estimate a property of f(x). The values of x can be treated as simulated measurements and from those, the probability of x taking values in certain region can be estimated.

Formally, the calculation of the Montecarlo simulation is simply an integration. In general, for one-dimensional integrals its viable to use other optimized numerical methods.

2.2. Taguchi's orthogonal array testing (TOAT) method

The fundamental part of this method consists in the optimization of products and processes, with the finality of guarantying robust products, with high quality and low costs. This is based in three steps:

- Design of the system.
- Design of the parameters.
- Design of tolerances.

From these three steps the most important one is the design of parameters; its main objectives are:

- Identify which factors affect the characteristics of quality when it comes to magnitude and variability.
- Define the "optimal" values than must be selected for each parameter or factor, to optimize the functionality of the product and make it as robust as possible.
- Identify factors that do not cause a substantial effect in the characteristic of quality to release the control of these factor and save in the testing costs.

To accomplish this, a series of statistical tools known as experiment design has been achieved. The TOAT presents an alternative not completely different to what is known as: orthogonal arrays and lineal graphs. The tool normally used is the fractionate factorial designs, however, when the number of factors increases, the possible interactions increase, just as the complications to identify which are the specific conditions needed to trial.

A Taguchi's matrix arrangement can be compared with a replication of a fractioned factorial, which conserves the concept of orthogonality and contrasts. A fractioned factorial trial is also an orthogonal arrangement. For a system with some uncertain input variables, the proper adjustment in control variables can make that the system adapts to different operating scenarios less sensitive to aleatory variables. Generally, some selected scenarios for uncertain variables are tested to guide the adjustment of the control variables.

Let us suppose that a system Y that can be represented by the function $Y = Y(x_1, \ldots, x_f)$ where $x_1, \ldots, x_f$ are F uncertain variables. If all the variables in the set $(x_1, \ldots, x_f)$ is represented by B levels and selecting its variable range, the number of all the combinations of the state of the system is BF. This is computationally expensive for all the BF testing in cases when F is too broad. Therefore, TOAT, is used to generate an optimal number of test scenarios and only a small number of tests are completed.

In TOAT, the testing scenarios are made according the Orthogonal Matrix (OM). An OM for F variables and B levels is represented by LH(BF), where H is the number of combinations of the variables. LH (BF) is represented in a matrix with H rows and F columns, the levels of the variable are indicated by the values inside the elements of the matrix. For example, in (1) OM L4(23) is represented.

$$L_4\left(2^3\right) = \begin{bmatrix} 1 & 1 & 1 \\ 1 & 2 & 2 \\ 2 & 1 & 2 \\ 2 & 2 & 1 \end{bmatrix} \tag{1}$$

Therefore, for the system Y, H scenarios can be made based on a OM LH(BF). Generally, H is much smaller than BF. For the (2.1) system, with three aleatory variables and each one represented by 2 levels, the number of all combinations is 23. However, according to L4(23), only 4 testing scenarios are made. Therefore, the number of testing is minimized. An OM has the following characteristics:

- For the variable in each column all the levels happen H/B times. For example, in L4(23), H = 4 and B = 2, which means that 1 and 2 happens twice in each column.
- In any of the columns, the combination of variables is produced the same number of times. For example, in any of the columns of L4(23), the combination of two levels of variable "11". "12", "21", and "22" appear once.
- The combinations determined by the OM are uniformly distributed in the space of all possible combinations. For example, the combination of the L4(23) are shown in Fig. 1.

The vertices of black color in Fig. 1 correspond to the L4(23) combinations.

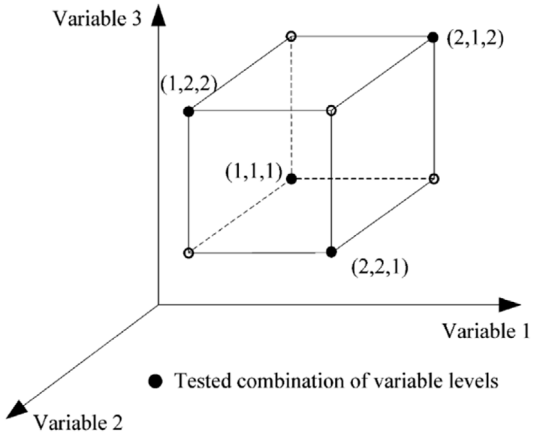

Fig. 1. Orthogonal matrix L4 (23).
Source: Own elaboration with data from [17].

According to the notation used by Taguchi in the arrangement used as an example, it is called L4 arrangement because it has four lines. In general, for a two-level arrangement, the number of columns (effects or factors) that can be analyzed is equal to the number of lines minus 1. Taguchi developed a series of arrangements for experiments with two level factors, the most used and spread ones according to the number of factors analyzed are given in Table 1.

Table 1. The notation of Taguchi's arrangements.
Source: Own elaboration with data from [17].

Number of factors to analyze	Fix to use	Number of conditions to be tested
Between 1 and 3	L4	4
Between 4 and 7	L8	8
Between 8 and 11	L12	12
Between 12 and 15	L16	16
Between 16 and 31	L32	32
Between 32 and 63	L64	64

2.3. Two-point estimation method for probability moments

X and Y being real aleatory variables and a function $Y = Y(X)$. Given the expected value of X and $\overline{X}$, the asymmetry coefficient v_x of X, and the standard deviationσ_x, approximate expressions are searched for the

distribution moments of X. The expressions are valid for all distributions of X, and the expressions of probability density functions (2) and (3) are selected.

$$P_+ \partial \left(\overline{X} - x_+\right) \tag{2}$$

$$P_- \partial \left(\overline{X} - x_-\right) \tag{3}$$

where P_+ and P_- are coefficients, ∂ is delta of Dirac and, x+ and x− are specific values of X. The probability density function consists of the concentrations P_+ y P_- in x+ and x−, respectively. Also, when Y admits and expansion in Taylor series on $\overline{X}$, now you obtain the expression (4).

$$E\left[Y^n\right] = P_+ y_+^n + P_- y_-^n \tag{4}$$

where $E[Y^n]$ is the expected value of the superior terms of the series, being $y_\pm = y(x_\pm)$, and n is a real number. From Eq. (4) the parameters of the distribution of Y can be determined.

$P_\pm y\ x_\pm$ must satisfy the simultaneous equations (5)–(8) to meet the following conditions.

$$P_+ + P_- = 1 \tag{5}$$

$$P_+ x_+ + P_- x_- = \overline{X} \tag{6}$$

$$P_+ \left(x_+ - \overline{X}\right)^2 + P_- \left(x_- - \overline{X}\right)^2 = \sigma_x^2 \tag{7}$$

$$P_+ \left(x_+ - \overline{X}\right)^3 + P_- \left(x_- - \overline{X}\right)^3 = \sigma_x^3 v_x^3 \tag{8}$$

Which is a solution for the terms (9)–(11).

$$P_+ = \frac{1}{2}\left[1 \mp \sqrt{1 - \frac{1}{(^V x/_2)^2}}\right] \tag{9}$$

$$P_- = 1 - P_+ \tag{10}$$

$$x = \overline{X} \mp \sigma_x \sqrt{\frac{P_\mp}{P_\pm}} \tag{11}$$

When v_x is insignificant and the probability distribution of X is approximately Gaussian, often the accuracy can be improved by taking the probability density to be concentrated in more that two points. For the negative values of v_x Eq. (12) will be applied.

$$P_+ = \frac{1}{2} - \frac{v_x}{4} \tag{12}$$

When v_x is unknown, this can be taken as null, then $P_\pm = 1/2$ and $x_\pm = \overline{X} \pm \sigma_x$. In this case Eq. (4) becomes (13)

$$\overline{Y} = \frac{y_+ + y_-}{2} \tag{13}$$

With the resulting terms (14) and (15):

$$\sigma_Y = \left|\frac{y_+ - y_-}{2}\right| \tag{14}$$

$$v_Y = \left|\frac{y_+ - y_-}{y_+ + y_-}\right| \tag{15}$$

To visualize, Fig. 2 presents the magnitudes of the concentrations for aleatory variables X1 and X2. Also, Fig. 3 is presented for the case of three stochastic variables.

As an example, for the described for this method, we have: consider the function $Y = X^k$, where the distribution of X is Log is normal with $\overline{X} = 1$ and $v_x = 0.2$. The exact parameters of the distribution of Y are given by (16) and (19).

$$\overline{Y} = \overline{X}^k \left(1 + v_x^2\right)^{k(k-1)/2} \tag{16}$$

$$1 + v_Y^2 = \left(1 + v_x^2\right)^{k^2} \tag{17}$$

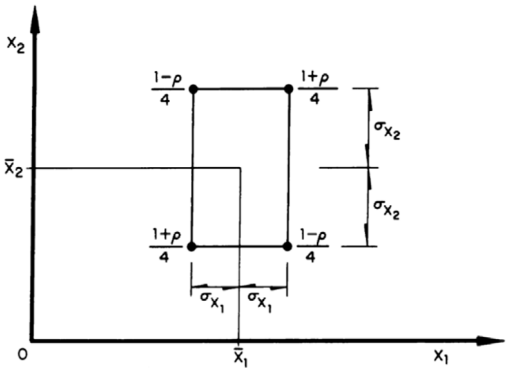

Fig. 2. Concentrations of the probability distribution function when $Y = Y(X_1, X_2)$.
Source: Own elaboration with data from [18].

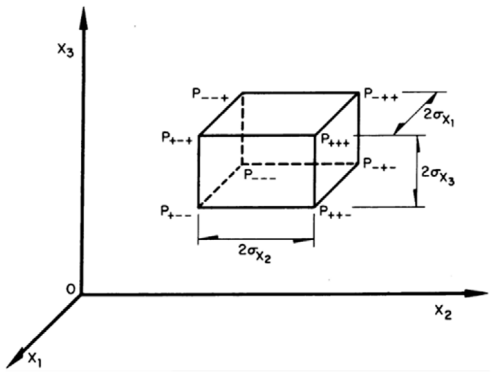

Fig. 3. Concentration of the probability distribution function when $Y = Y(X_1, X_2, X_3)$.
Source: Own elaboration with data from [18].

By deduction:

$$E\left[\left(X-\overline{X}\right)^3\right] = \overline{X}^3 v_x^4 \left(3+v_X^2\right) \tag{18}$$

Therefore,

$$v_x = v_x\left(3+v_x^2\right) = 0.608 \tag{19}$$

According to Eqs. (9)–(11), P+ = 0.35457, … with k = 3 the exact answer is according to Eqs. (16) and (17), $\overline{Y} = 1.125$, $v_y = 0.651$. The Eq. (4) has the same value than $\overline{Y}$ y$v_y = 0.693$, while according to the Eqs. (13)–(15), $\overline{Y} = 1.120$, $v_y = 0.543$.

3. IEEE test system of 13 nodes

In Fig. 4 shows the one-line diagram of the test system used for this study.
This power system is integrated by the following elements and electric conditions:

- 2 bars with generations, located in the 650 and 680 nodes.
- The 650 bar is taken as “slack”. The wind and solar units generating the generation uncertainty are located in the 680 bar.
- 9 bars PQ, located in the nodes: 632, 671, 646, 645, 634, 611, 692, 675 y 652. These produce an uncertainty due to the changes in the demand of real power and reactivate at different times of the day and 12 branches that build the network between the different nodes.
- It is assumed that the transmission lines behave ideally to not the chargeability of these.

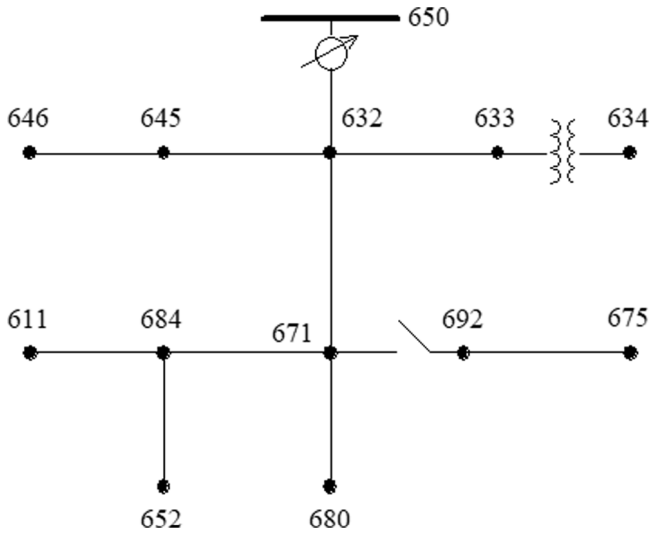

Fig. 4. One-line diagram for the IEEE system of 13 nodes.
Source: Own elaboration with data from IEEE.

For the purposes of this study it will be assumed that the IEEE system of 13 nodes is in balance between its phases and it will be able to perform the calculation of the power flow in MATPOWER in an optimal way.

Table 2 shows the wind speed for El Cabo de la Vela-Guajira for 2017.

Table 2. Wind speed for El Cabo de la Vela, Guajira, Colombia, 2017.
Source: Own elaboration with data from NASA.

Month	Wind m/s
January	7,7
February	7,9
March	7,7
April	6,4
May	5,5
June	6,5
July	6,7
August	5,7
September	4,6
October	4,4
November	5,2
December	6,9

Table 3 shows the solar radiation data for Bogota City, Colombia for 2017.

4. Results

The Weibull function is a function characterized by two parameters. One of them is the scale and the other is the shape. The first one defines how disperse the distribution is while the second one defines the shape of the distribution. The Weibull probability of density is given by:

$$f(v) = \left(\frac{k}{c}\right)\left(\frac{v}{c}\right)^{k-1} exp\left[-\left(\frac{v}{c}\right)^{k}\right] \tag{20}$$

And the function of accumulated distribution is:

$$F(v) = 1 - exp\left[-\left(\frac{v}{c}\right)^{k}\right] \tag{21}$$

Table 3. Solar radiation in Bogota City, Colombia, 2017.
Source: Own elaboration with data from NASA.

Month	Daily solar radiation kWh/m^2-day
January	4,86
February	4,83
March	4,91
April	4,65
May	4,72
June	4,83
July	5,00
August	5,07
September	5,03
October	4,7
November	4,6
December	4,6

The values used for the wind speeds belong to El Cabo de la Vela-Guajira in 2017, were obtained from the NASA website. With this data the Maximum Probability method was applied by using the following equations:

$$k = \left(\frac{\sum_{i=1}^{N} v_i^k ln\,(v_i)}{\sum_{i=1}^{N} v_i^k} - \frac{\sum_{i=1}^{N} ln\,(v_i)}{N} \right)^{-1} \tag{22}$$

$$c = \left(\frac{1}{N} \sum_{i=1}^{N} v_i^k \right)^{1/k} \tag{23}$$

where N represents the number of observations and vi the average wind speed registered in that time frame.

Fig. 5 shows probability curve of the wind speed for El Cabo de la Vela, Guajira for 2017 and Fig. 6 shows the function of accumulated distributions of wind speed for the same year.

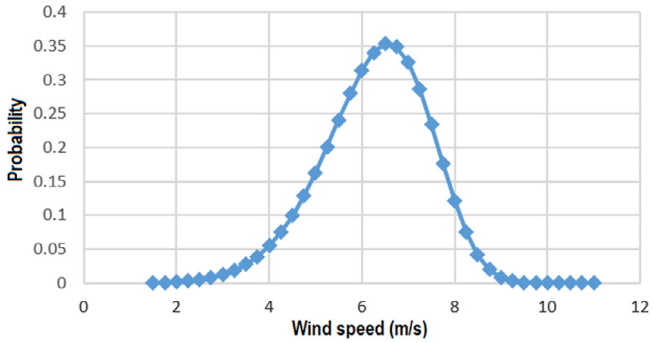

Fig. 5. Probability curve for the wind speed for El Cabo de la Vela, Guajira, 2017.
Source: Own elaboration.

The values of shape and scale of the wind speed for El Cabo de la Vela, Guajira found with the use of Matpower are: K = 6,39534069 and y C = 6,74360088. These values are introduced in the simulation of the Montecarlo method in the code designed in Matlab for power flows integrating the uncertainty of the wind speed in the IEE test system of 13 nodes.

Fig. 7 shows the probability curve for the solar radiation in Bogota City in 2017 and Fig. 8 presents the function of accumulated distribution of solar radiation for the same year.

As seen in Fig. 7, Bogota has excellent solar radiation conditions for the production of electricity. The highest probabilities of photovoltaic generation have solar radiation greater than 4, 5 kWh/m^2-day; which can be contrasted with the cumulative distribution function shown in Fig. 8.

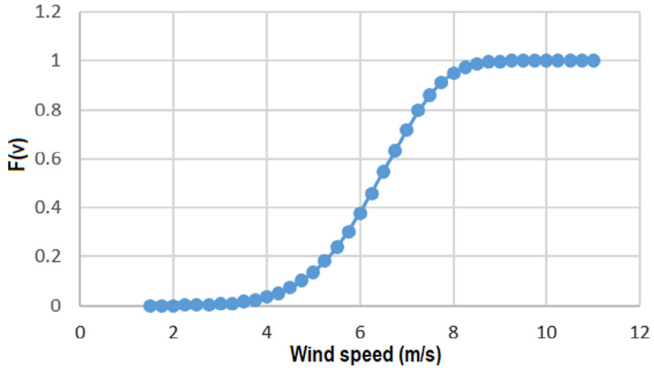

Fig. 6. Function of accumulated distributions of wind speed for El Cabo de la Vela, Guajira, 2017. *Source:* Own elaboration.

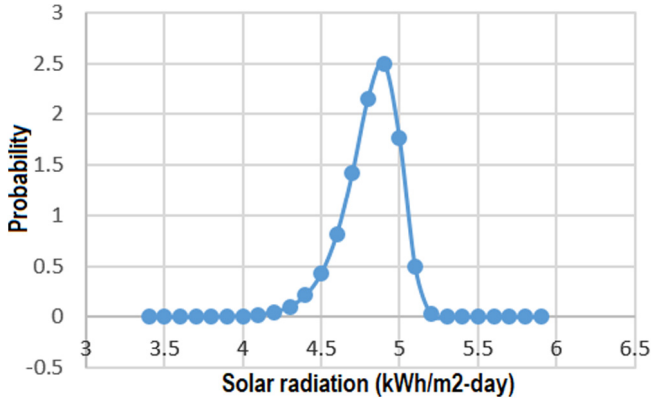

Fig. 7. Probability curve for the solar radiation in Bogota, Colombia, 2017. *Source:* Own elaboration.

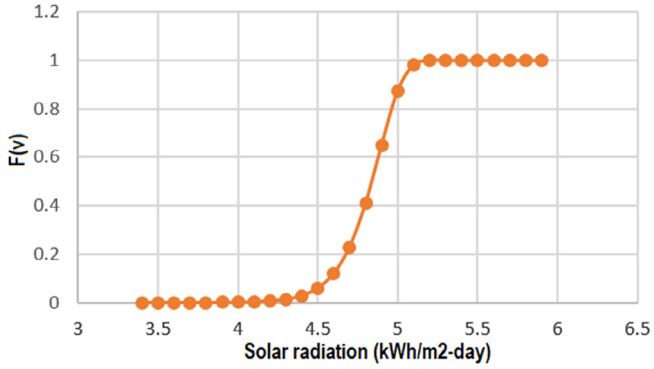

Fig. 8. Function of accumulated distribution of solar radiation in Bogota, Colombia, 2017. *Source:* Own elaboration.

The values of shape and scale of solar radiation found using the MP method are: K = 33,359 y C = 4,8937. These values are input in the simulation of the Montecarlo method in the code designed in Matlab for power flows integrating the uncertainty of solar radiation in the IEEE system of 13 nodes.

4.1. Modeling the wind speed and solar radiation

The Montecarlo simulation for the wind speed at El Cabo de la Vela, Guajira fulfilled the following conditions of probability distribution:

- The loads were simulated as uniform probability distributions that vary between 70% and 120% of the nominal real power demanded by each node.
- The uncertain variable generated by the wind system is simulated as a Weibull probability distribution with parameters of shape and scale of 6,3953 and 6,7436.
- Size of the sample = 10.000 data.
- Time of simulation: 97,145832 s.

The TOAT simulation for the wind speed at El Cabo de la Vela, Guajira, considered the following criteria for the construction of the OM:

- Uncertain variables: 1 of renewable generation plus 9 of uncertain loads. F = 10 the uncertain variables.
- The number of levels inside each element of the matrix is selected. For this study there is going to be 2 levels: B = 2.
- An OM is selected with columns equal to F. since there is not a defined OM with this number of columns, L12(211) is selected. The first six columns are used for this study.
- L8 indicates that there will be 12 testing scenarios in each OM.

Different combinations can be generated between the values assigned to 1 and 2 for its maximum and minimum values, as showed in Table 4.

Table 4. Taguchi orthogonal matrix.
Source: Own elaboration.

Orthogonal matrix number	Level number	Assigned renewable generation [%]	Load value [%]
OM1	1	25	120
	2	100	70
OM2	1	100	70
	2	25	120
OM3	1	25	70
	2	100	120
OM4	1	100	120
	2	25	70

Size of the sample = 48 scenarios.
Time of simulation = 0,595136 s.
Each OM has 12 different testing scenarios and when 4 possible combinations are built between 1 and 2, we can obtain 48 different testing scenarios, which were programmed in only a 48 × 11 matrix.

The simulation using the two-point estimation method for the wind speed at El Cabo de la Vela, Guajira, considered the maximum and minimum values of the active powers demanded in each bar of the IEEE system of 13 nodes as follows:

- Load 1(Bus 632) = Max = 0.100 MW * 1,2 = 0.12 MW, Min = 0.100 MW * 0,7 = 0.07 MW
- Load 2(Bus 671) = Max = 0.385 MW * 1.2 = 0.46 MW, Min = 0.385 MW * 0,7 = 0.26 MW
- Load 3(Bus 646) = Max = 0.230 MW * 1,2 = 0.27 MW, Min = 0.230 MW * 0,7 = 0.16 MW
- Load 4(Bus 645) = Max = 0.170 MW * 1,2 = 0.20 MW, Min = 0.170 MW * 0,7 = 0.11 MW
- Load 5(Bus 634) = Max = 0.160 MW * 1,2 = 0.19 MW, Min = 0.160 MW * 0,7 = 0.11 MW
- Load 6(Bus 611) = Max = 0.170 MW * 1,2 = 0.20 MW, Min = 0.170 MW * 0,7 = 0.11 MW
- Load 7(Bus 692) = Max = 0.170 MW * 1,2 = 0.20 MW, Min = 0.170 MW * 0,7 = 0.11 MW
- Load 8(Bus 675) = Max = 0.485 MW * 1,2 = 0.58 MW, Min = 0.485 MW * 0,7 = 0.33 MW
- Load 9(Bus 652) = Max = 0.128 MW * 1,2 = 0.15 MW, Min = 0.128 MW * 0,7 = 0.08 MW

The statistics for each load in active energy demand are summarized in Table 5.

Table 5. Statistic of the probability distribution functions of the loads (active power).
Source: Own elaboration.

Node	Nominal active power [MW]	Half	Median	Standard deviation	Variance	Bias	Coefficient of variation	Minimum value	Maximum value
632	0.100	0.10	0.10	0.01	0.00	0.00	0.1519	0.07	0.12
671	0.385	0.36	0.36	0.06	0.00	0.00	0,1604	0.26	0.46
646	0.230	0.22	0.22	0.03	0.00	0.00	0,1477	0.16	0.27
645	0.170	0.16	0,16	0.03	0.00	0.00	0.1676	0.11	0.20
634	0.160	0.15	0.15	0.02	0.00	0.00	0.1540	0.11	0.19
611	0.170	0.16	0.16	0.03	0.00	0.00	0.1676	0,11	0.20
692	0.170	0.16	0.16	0.03	0.00	0.00	0.1676	0.11	0.20
675	0.485	0.46	0.46	0.07	0.01	0.00	0.1586	0.33	0.58
652	0.128	0.12	0.12	0.02	0.00	0.00	0.1757	0.08	0.15

Knowing these values, apply the equations from Section 2.3. to find the maximum and minimum generation values in the bar 2.

Since the bias is negative Eq. (12) is applied, resulting in the expressions (24)–(25).

$$V_x = -0.4116 \tag{24}$$

$$x = \overline{X} \overline{+} \sigma_x \sqrt{\frac{P_{\overline{+}}}{P_{\pm}}} \Rightarrow \begin{cases} x_+ = 1.65 \text{ MW} \\ x_- = 1.11 \text{ MW} \end{cases} \tag{25}$$

Considering these values, the arithmetic mean is calculated:

$$\overline{X} = \frac{(1.65 + 1.11)}{2} = 1.38 \text{ MW} \tag{26}$$

Size of the sample = 1024 scenarios.

Time of simulation: 314,737494 s.

The Montecarlo simulation for the solar radiation in Bogota, fulfilled the following conditions of probability distribution in each uncertain variable:

- The loads were simulated as uniform probability distributions that vary between 70% and 120% of the nominal real power demanded by each node.
- The uncertain variable generated by the photovoltaic system is simulated as a Weibull probability distribution with parameters of shape and scale of 33,36 y 4,89.
- Size of the sample = 10.000 scenarios.
- Time of simulation: 98,8380 s.

The simulation using the TOAT method for the solar radiation for Bogota city, considered the following criteria for the construction of the OM:

- Uncertain variables: 1 of renewable generation plus 9 of uncertain loads. F = 10 the uncertain variables.
- The number of levels inside each element of the matrix is selected. For this study there is going to be 2 levels: B = 2.
- An OM is selected with columns equal to F. since there is not a defined OM with this number of columns, L12(211) is selected. The first ten columns are used for this study.
- L8 indicates that there will be 12 testing scenarios in each OM.

Size of the sample = 48 scenarios.

Time of simulation: 0,595136 s.

The simulation using the Two-point estimation method for solar radiation in Bogota, considered a Weibull distribution to find the maximum and minimum values of generation in the bar 2.

Since the bias is negative Eq. (12) is applied, resulting in the expressions (27)–(28).

$$V_x = -0.9708 \tag{27}$$

$$x = \overline{X} \mp \sigma_x \sqrt{P_{\mp}/P_{\pm}} \Rightarrow \begin{cases} x_+ = 1.13 \text{ MW} \\ x_- = 1.03 \text{ MW} \end{cases} \tag{28}$$

Considering these values, the arithmetic mean is calculated:

$$\overline{X} = \frac{(1.13 + 1.03)}{2} = 1.08 \text{ MW} \tag{29}$$

Size of the sample = 1024 scenarios.
Time of simulation: 315,275230 s.

4.2. Statistical results for wind speed and solar radiation

Fig. 9 Shows the voltage box (p.u) graph for the wind generation (El Cabo de la Vela, Guajira) using the Montecarlo method in the IEEE system of 13 nodes.

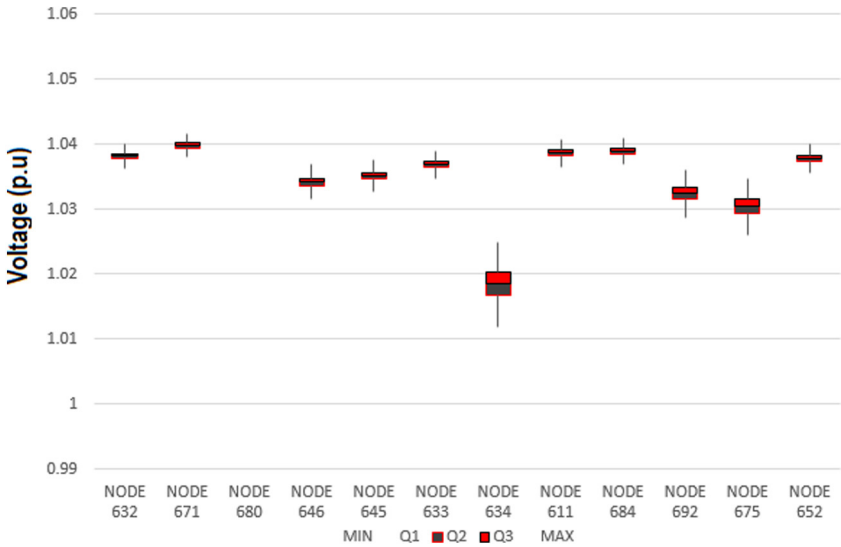

Fig. 9. Graph of the voltage box (p.u) for the wind generation at El Cabo de la Vela, using the Montecarlo method.
Source: Own elaboration.

Voltage variation using the Montecarlo method for the entire system was recorded between 1,012 p.u (node 634) and 1,042 p.u (node 671). Particularly in the node 634, the voltage range was 0,013 p.u (data vary between 1,012 p.u. and 1,025 p.u.) with a median of 1,0185 p.u. for the rest of the nodes of the testing system, the integration of the wind generation does not alter the voltage by no more than 0,046 p.u. with the node 671 presenting the highest magnitude.

Fig. 10 shows the graph of the voltage box (p.u.) for the wind generation (at El Cabo de la Vela, Guajira) using the TOAT method in the IEEE system of 13 nodes.

In the case of the TOAT method, the wind generation in the testing systems makes the voltage vary in a range of 0,044 p.u. for the node 634, the TOAT method produces a lower distribution of the whiskers compared to the Montecarlo method. Specifically, the first quarter of the voltage of the node 634 varies between 1,023 p.u. and 1,025 p.u. while the last quarter varies between 1,085 p.u. and 1,011 p.u. with a median of 1,017 p.u.

Fig. 11 shows the graph of the voltage box (p.u.) for the wind generation (at El Cabo de la Vela, Guajira) using the two-point method in the IEEE system of 13 nodes.

The simulation of the algorithm of the two-point method generates the variability of the voltage lower to 1,04 p.u. for the nodes of the system and higher to 1,012 p.u. The variability of the voltage data of the box graph for each node using this method is the lowest compared to the two previous methods.

The results for the wind generation suggest a careful and independent evaluation for each one of the nodes in the system, there is an evident alteration in the voltage for node 634 under the normal behavior of the other nodes.

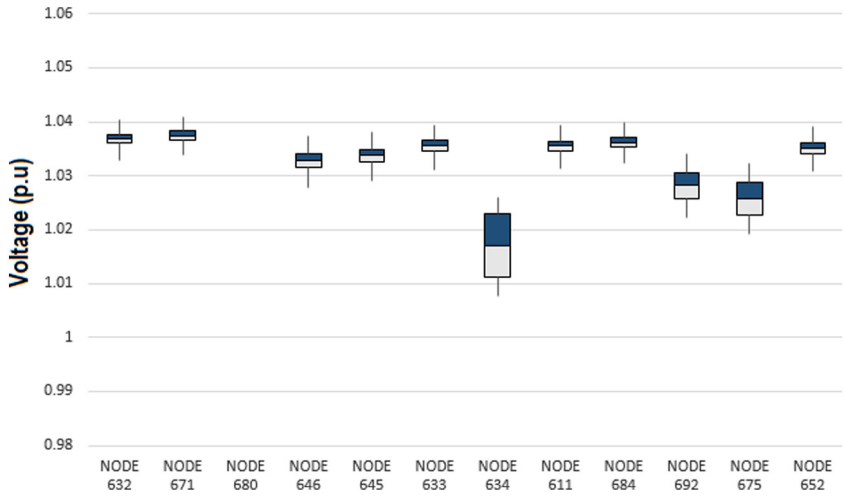

Fig. 10. Graph of the voltage box (p.u.) for the wind generation at El Cabo de la Vela using the TOAT method. *Source:* Own elaboration.

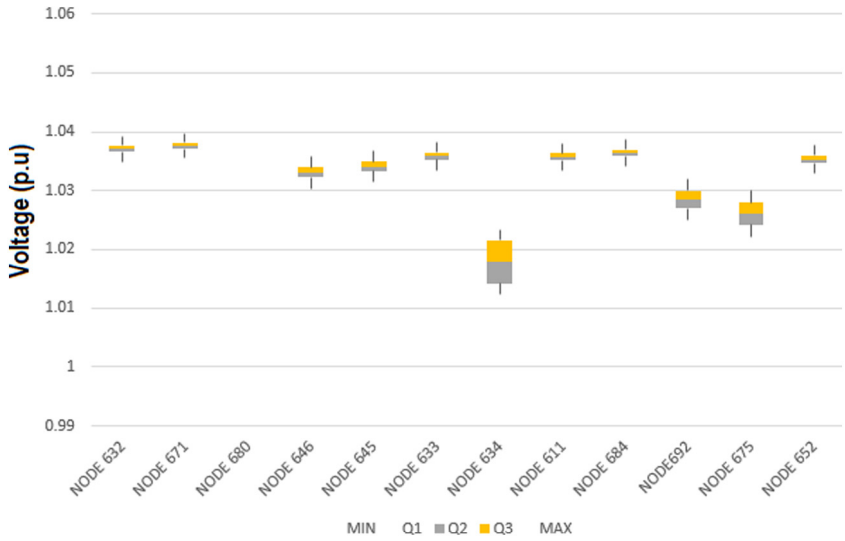

Fig. 11. Graph of the voltage box (p.u.) for the wind generation at El Cabo de la Vela using the two-point method. *Source:* Own elaboration.

Fig. 12 shows the demanded active power (p.u.) of wind power in each node using the TOAT method.

As observed in Fig. 12 the results do not generate whiskers in the box graph, using the TOAT method, which indicates that this method does not select random values but calculates them deterministically assuming maximum and minimum values for each variable.

The nodes that demand a higher amount of wind power are the nodes 671, 646 and 675. The wind power demanded by node 671 has a median of 0,367 p.u. with a minimum of 0,275 p.u. and a maximum of 0,466 p.u. while the node 675 presents a demanded wind power with a median of 0,462 p.u. and its range varies between 0,333 p.u. and 0,587 p.u.

Fig. 13 shows the voltage box graph (p.u) for the photovoltaic generation in Bogota using the Montecarlo method in the IEEE system of 13 nodes.

The voltage variation using the Montecarlo method for the photovoltaic generation presented the same results as for wind generation: between 1,012 p.u (node 634) and 1,042 p.u (node 671).4

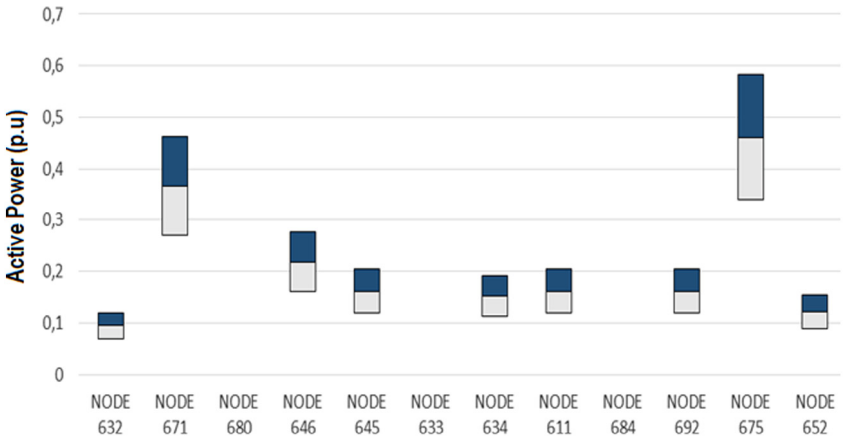

Fig. 12. Graph of the box of the active power demanded in p.u. of wind energy, using TOAT method for El Cabo de la Vela, Guajira. *Source:* Own elaboration.

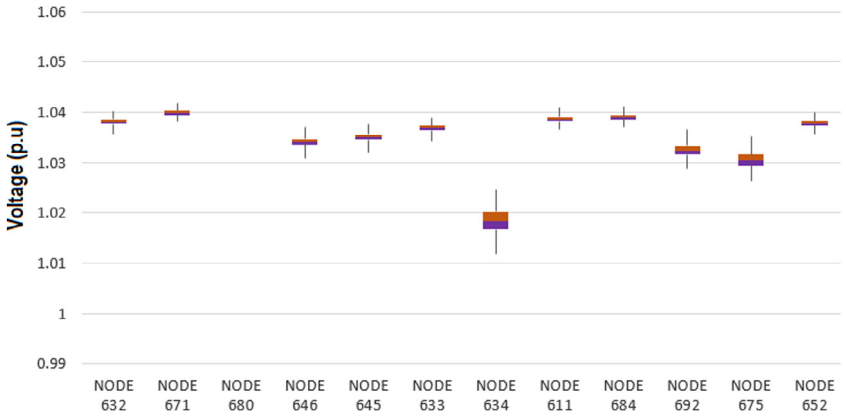

Fig. 13. Voltage box graph (p.u) for photovoltaic generation in Bogota using the Montecarlo method. *Source:* Own elaboration.

Both simulations (wind and photovoltaic generation) had the same sample size when using the Montecarlo method: 10,000 data. The difference was noticeable in the time taken for the simulation: 97,145832 s for the wind generation and 98,8380 s for the photovoltaic generation.

Fig. 14 shows the voltage box graph (p.u) for photovoltaic generation in Bogota using the TOAT method in the IEEE system of 13 nodes.

The generation of whiskers in the cash charts of the results indicate a probabilistic analysis of the applied methods. The node 634 presents a higher drop of voltage of the whole system: the lowest voltage reported was 1,097 p.u. and 1,025 p.u. and the highest was 1,025 p.u., with a 1,0175 p.u. median. Other node representing a drop in the voltage was the node 675 which registered a minimum of 1,019 p.u.

The TOAT method behaves identically in the two cases analyzed (solar and wind), since this always takes the "maximum" and "minimum" of each variable. Also, with both resources the same installed generation capacity was assumed (1.65 MW), with 100% being the maximum and the minimum of 25% of capacity.

Fig. 15 shows the voltage box graph (p.u) for photovoltaic generation (in Bogota) using two-point method in the IEEE system of 13 nodes.

Again, for this case the probabilistic behavior of the results are similar to those reported for the wind generation of Fig. 11. The results for the two-point method generates a variability of the voltage lower than 1,04 p.u. for all the nodes in the system and higher than 1,012 p.u.

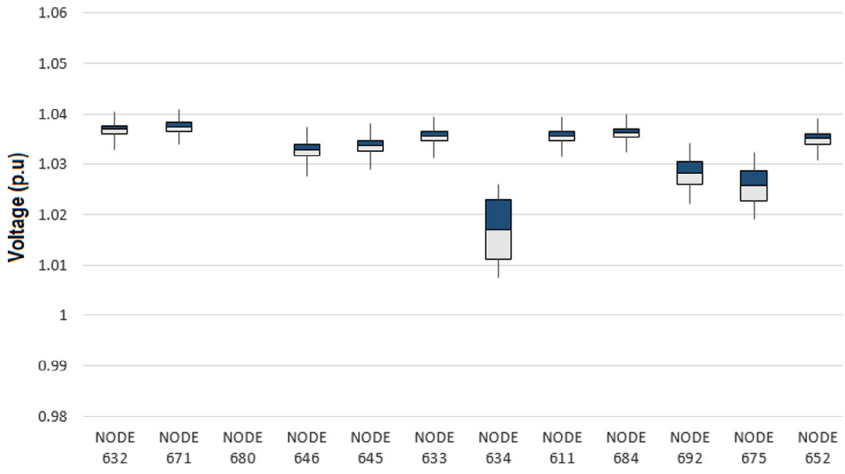

Fig. 14. Voltage box graph (p.u) for photovoltaic generation in Bogota using the TOAT method. *Source:* Own elaboration.

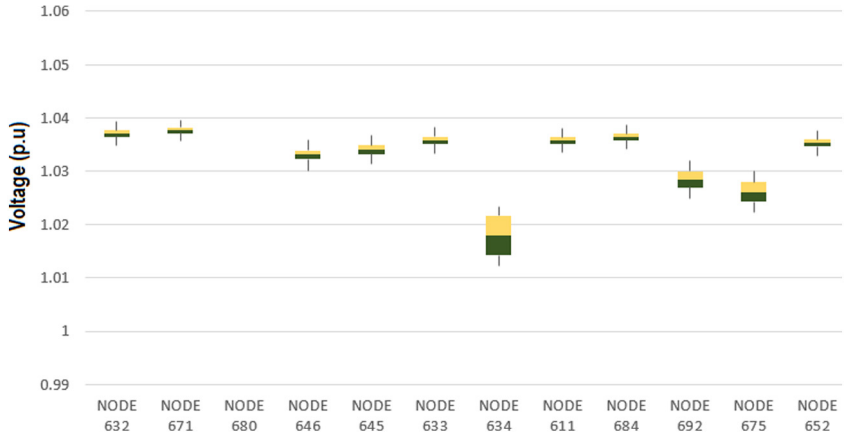

Fig. 15. Voltage box (p.u) for photovoltaic generation in Bogota, using the two-point method. *Source:* Own elaboration.

Fig. 16 shows the demanded active power (p.u) of solar energy in Bogota in each node using the two-point method.

In this simulation whiskers are not obtained in the box graphs, just like it happened with the TOAT method applied to the wind generation in Fig. 12. Also, because of the deterministic calculation made by the two-point method: the sum of the standard deviation and the means as initial values of each variable (generation and charge). The nodes with higher photovoltaic demand were node 671 with a maximum power of 0,423 p.u. and the node 675 which registered a median of 0,46 p.u.

5. Conclusions

In the Montecarlo and two-point methods, the Weibull probability distribution function is considered the primary to represent the variable behavior of the wind and solar resources; which determines the probabilistic nature of these methods. On the other hand, the TOAT method does not leave any random variable, taking only the maximum and minimum levels of each one to perform the different iteration, being merely a deterministic method.

The TOAT method improves its behavior if the number of levels is increased for each variable, not only taking the maximum and minimum levels but incorporating the intermediate levels.

Fig. 16. Cash graph of the active power demanded in p.u. of photovoltaic energy, using the two-point method for Bogota. *Source:* Own elaboration.

The number of iterations in each method varies: the TOAT and the two-point methods the number of iterations is related to the number of variables in the system, while in the Montecarlo method it remains to the choice of the programmer making the simulation. Considering that the more iterations are made in the Montecarlo method, the greater the precision of the probabilities obtained.

The two-point method has an advantage over the other two methods studied: the statistical characteristics of the PDF of the variables are considered to determine their initial values deterministically to then probabilistically iterate the different scenarios, which means it is a combination between the benefits of the deterministic and the probabilistic.

Funding

This work was supported by Universidad de Bogotá Jorge Tadeo Lozano, Colombia under Grant 830-15-17.

References

[1] Chinmoy Lakshmi, Iniyan S, Goic Ranko. Modeling wind power investments policies and social bene Fi Ts for deregulated electricity market – A review. Appl Energy 2019;242(May 2018):364–77. http://dx.doi.org/10.1016/j.apenergy.2019.03.088.

[2] Han Yutong, et al. A PV power interval forecasting based on seasonal model and nonparametric estimation algorithm. Sol Energy 2019;184(February):515–26. http://dx.doi.org/10.1016/j.solener.2019.04.025.

[3] Georgitsioti Tatiani, Pearsall Nicola, Forbes Ian, Pillai Gobind. A combined model for PV system lifetime energy prediction and annual energy assessment. Sol Energy 2019;183(July 2018):738–44. http://dx.doi.org/10.1016/j.solener.2019.03.055.

[4] Kushwaha Vishal, Pindoriya Naran M. A SARIMA-RVFL hybrid model assisted by wavelet decomposition for very short-term solar PV power generation forecast. Renew Energy 2019;140:124–39. http://dx.doi.org/10.1016/j.renene.2019.03.020.

[5] Yan J, et al. Uncertainty estimation for wind energy conversion by probabilistic wind turbine power curve modelling. Appl Energy 2019;239(February):1356–70.

[6] Seo Seokho, Oh Si-doek, Kwak Ho-young. Wind turbine power curve modeling using maximum likelihood estimation method. Renew Energy 2019;136:1164–9. http://dx.doi.org/10.1016/j.renene.2018.09.087.

[7] Ali Moazam, Bagchi Susmit. Probabilistic normed load monitoring in large scale distributed systems using mobile agents. Future Gener Comput Syst 2019;96:148–67. http://dx.doi.org/10.1016/j.future.2019.01.053.

[8] Karmellos M, Georgiou PN, Mavrotas G. A comparison of methods for the optimal design of distributed energy systems under uncertainty. Energy 2019;178:318–33. http://dx.doi.org/10.1016/j.energy.2019.04.153.

[9] Kumar NM, Gupta RP, Mathew M, Jayakumar A, Singh NK. Performance, energy loss and degradation prediction of roof-integrated crystalline solar PV system installed in northern India. Case Stud Therm Eng 2019;13:100409.

[10] Anastasiadis Anestis G, et al. Maximum power photovoltaic units penetration under voltage power photovoltaic units penetration under voltage constraints criteria in distribution network using probabilistic constraints criteria in distribution network using probabilistic load flow the heat demand-outdoor assessing the feasibility of using load flow temperature function for a long-term district heat demand forecast kondylis. Energy Procedia 2019;157(2018):578–85. http://dx.doi.org/10.1016/j.egypro.2018.11.222.

[11] Uniyal Ankit, Kumar Ashwani. Optimal distributed generation placement with multiple objectives optimal distributed generation placement with multiple objectives considering probabilistic load considering probabilistic load. Procedia Comput Sci 2018;125(2017):382–8. http://dx.doi.org/10.1016/j.procs.2017.12.050.

[12] Andri I, Pina A, Ferrão P. Probabilistic energy flow analysis for urban energy systems probabilistic energy flow analysis for urban energy systems considering correlated uncertainties considering correlated uncertainties assessing the feasibility of using the heat temperature function for a district heat demand forecast. Energy Procedia 2019;158:6472–7. http://dx.doi.org/10.1016/j.egypro.2019.01.120.

[13] Kang Jing, Wang Shengwei. Robust optimal design of distributed energy systems based on life-cycle performance analysis using a probabilistic approach considering uncertainties of design inputs and equipment degradations. Appl Energy 2018;231(September):615–27. http://dx.doi.org/10.1016/j.apenergy.2018.09.144.

[14] Chauhan Ranchan, et al. Experimental investigation and optimization of impinging jet solar thermal collector by Taguchi method. Appl Therm Eng 2017;116:100–9. http://dx.doi.org/10.1016/j.applthermaleng.2017.01.025.

[15] Li C, Qinge X, Li L. A method integrating Taguchi, RSM and MOPSO to CNC machining parameters optimization for energy saving. J Cleaner Production 2016;135:263–75.

[16] Singh Paramjit, Singh Sehijpal, Kumar Raman. Optimization of energy consumption response parameters for turning operation using Taguchi method. J Cleaner Prod 2016;137:1406–17. http://dx.doi.org/10.1016/j.jclepro.2016.07.220.

[17] Han Y, Chung CY, Wong KP. Robust transmission network expansion planning method with Taguchi's orthogonal array testing. IEEE Trans Power Syst 2011;26(3):1573–80.

[18] Rosenblueth E. Point estimates for probability moments. Proc Nat Acad Sci 1975;72(10):3812–4.